World Academy of Science, Engineering and Technology
International Journal of Mechanical and Mechatronics Engineering
Vol:8, No:3, 2014

Model-Based Control for Piezoelectric-Actuated Systems Using Inverse Prandtl-Ishlinskii Model and Particle Swarm Optimization

Jin-Wei Liang, Hung-Yi Chen, Lung Lin

Open Science Index, Mechanical and Mechatronics Engineering Vol:8, No:3, 2014 publications.waset.org/9997810/pdf

***Abstract*—**In this paper feedforward controller is designed to eliminate nonlinear hysteresis behaviors of a piezoelectric stack actuator (PSA) driven system. The control design is based on inverse Prandtl-Ishlinskii (P-I) hysteresis model identified using particle swarm optimization (PSO) technique. Based on the identified P-I model, both the inverse P-I hysteresis model and feedforward controller can be determined. Experimental results obtained using the inverse P-I feedforward control are compared with their counterparts using hysteresis estimates obtained from the identified Bouc-Wen model. Effectiveness of the proposed feedforward control scheme is demonstrated. To improve control performance feedback compensation using traditional PID scheme is adopted to integrate with the feedforward controller.

***Keywords*—**The Bouc-Wen hysteresis model, Particle swarm optimization, Prandtl-Ishlinskii model.

I. Introduction

CONTROL of a micro-/nanopositioning mechanism actuated by piezoelectric stack actuator (PSA) is investigated here. Compared with other types of actuators, PSA is capable of positioning with nanometer resolution and rapid response. Nevertheless, PSA also exhibits undesired nonlinear hysteresis behaviors. Hysteresis feature of the PSA manifests itself as a loop structure between the input voltage and output displacement where the ascending characteristics are different from the descending ones. Hysteresis also causes severe open-loop positioning error that can be as high as 10-15% of the span of the motion. Thus, the hysteresis effect has to be suppressed in high-precision application scenarios [1]-[5]. To alleviate hysteresis, model-based control can be adopted. However, modeling the hysteresis is a nontrivial task because such nonlinearity is not only amplitude but also frequency dependent. Generally, the hysteresis is modeled using Preisach model [6], Prandtl-Ishlinskii (P-I) model [7], Bouc-Wen model [8]-[10], etc. When precise mathematical model is obtained, an inverse hysteresis model if it exists can be constructed and utilized as the feedforward control input to cancel hysteresis effect. This study identifies parameters ofthe P-I hysteresis model using particle swarm optimization (PSO) technique so that both the inverse P-I model and feedforward control can be constructed.

J.-W. Liang and H.-Y. Chen are faculty with the Department of Mechanical Engineering, Ming Chi University of Technology, (e-mail: liangj@mail.mcut.edu.tw; hychen@mail.mcut.edu.tw).

L. Lin is a graduate student with the Department of Mechanical Engineering, Ming Chi University of Technology, (e-mail: heat0614@hotmail.com).

Due to the highly nonlinear, high dimensional, non-differential and multiple constraint nature, the identification of the P-I model constitutes a challenging problem. To overcome this, particle swarm optimization (PSO) technique is adopted. PSO is a relatively new heuristic search method based on the idea of collaborative behavior and swarming in biological populations. Unlike conventional local search optimization methods such as the least squares method, intelligent algorithms which may not be so efficient in dealing with this case, PSO is a multi-agent parallel search technique [11]-[13]. Conceptually, each particle in PSO is equipped with a small memory comprising its previous best position. The latter includes the personal best experience and the best value so far in the group among the best positions. The "group best" is referred to as the globally best particle in the entire swarm. Hence, the potential solutions of PSO, or called trial particles, basically fly through the whole problem space attempting to settle down at an optimal position. The optimal position usually is defined by some sorts of optimization criterion which in identification problem is referred to a fitness function or the square sum of errors between outputs obtained from real system and the identified model.

II. Problem Statement

A. Prandtl-Ishlinskii model

The Prandtl-Ishlinskii (P-I) model has been widely applied to describe the hysteresis nonlinearity due to its reduced complexity in comparison with Preisach model and analytical form of the inversion [14]. The backlash operator is the primary operator of the P-I model which is defined as the following discrete form [5], [14]

$$y(k) = H_r[x, y_0](k) = \max\{x(k) - r, \min\{x(k) + r, y(k-1)\}\} \quad (1)$$

where x is the control input, y is the actuator response, r is the control input threshold value or the magnitude of the backlash. The initial consistency condition of (1) can be written as

$$y(0) = \max\{x(0) - r, \min\{x(0) + r, y_0\}\} \quad (2)$$

When complex hysteretic nonlinearity is facing, the hysteretic loop can be modeled by a linearly weighted superposition of many backlash operator with different threshold and weight values. Thus,

$$y(k) = \mathbf{w}^T \cdot \mathbf{H}_r[x, \mathbf{y}_0](k) \quad (3)$$

Open Science Index, Mechanical and Mechatronics Engineering Vol:8, No:3, 2014 publications.waset.org/9997810/pdf

where $\mathbf{w}^T = [w_1 \quad w_2 .... w_n]$, $\mathbf{y}_0 = [y_{01} \quad y_{02} .... y_{0n}]^T$, $\mathbf{H}_r[x, \mathbf{y}_0](k) = [H_{r1}[x, y_{01}](k) \quad ... \quad H_{rn}[x, y_{0n}](k)]^T$, with threshold vector $\mathbf{r} = [r_1 \quad r_2 ... \quad r_n]^T$; $0 = r_1 < r_2 < ..... < r_n$. The control input threshold values **r** are usually, but not necessarily, chosen as equal intervals. In this study they are determined using the following equation

$$r_i = \frac{(i-1)}{n+1} \max\{|x(t)|\}, \quad i = 1 \cdots n \tag{4}$$

Moreover, it is assumed that the hysteretic actuator starts in its de-energized state. Thus, $y_{0i} = 0, \quad i = 1 \cdots n$.

B. Particle Swarm Optimization

In PSO, particles are conceptual entities that fly through the multi-dimensional search space. At any particular instant, each particle possesses a position and velocity where the position vector of a particle represents a trial solution of the optimum problem. When implementing the searching algorithm, a population of particles is initialized with random positions denoted as $\mathbf{x}_i$ and random velocity $\mathbf{v}_i$. All particles are evaluated according to the predefined fitness function. Comparing the fitness value, each particle records its personal best experienced position as *pbest*$_i$, and the global best experienced position as *gbest*. Thus, the global version of PSO is implemented as the following steps [2]:

1. Initialize a population of particles with random positions and velocities in *d* dimensions where *d* represents the number of un-determined parameters.
2. Compute the value of fitness function in *d* variables for each particle.
3. For each particle, compare the fitness value with that of the *pbest*. If the current fitness value is better than that of the *pbest*, change the *pbest* value to the current value and change the *pbest* location to the current location in *d* dimensional space.
4. For each particle, compare the fitness value with the best value observed so far in the overall population. If the current value is better than *gbest*, reset the *gbest*to the current array index and value of current particle.
5. Update the velocity and position of the particle using the following equations

$$v_{ij}(k+1) = w v_{ij}(k) + c_1 r_1 [p_{ij}(k) - x_{ij}(k)] + c_2 r_2 [g_{ij}(k) - x_{ij}(k)] \tag{5}$$

$$x_{ij}(k+1) = x_{ij}(k) + v_{ij}(k+1), \quad j = 1,2,..d \tag{6}$$

where r_1 and r_2 are two random variables in the range of [0,1], c_1 and c_2 are acceleration coefficients, w is the inertia weight, $p_i(k)$ and $g_i(k)$ denote the positions of *pbest*and *gbest*, respectively.

6. Start over at step (2) unless a termination criterion is met. The termination criteria are usually a sufficiently good fitness value or the maximum number of iterations.

III. Hysteresis Modeling and Identification

A. Experimental Setup

The experimental setup consists of a PSA (Piezomechanik, PSt500/10/25), a flexible mechanism, a load cell (Honeywell, model 13) and a PC-based control unit with D/A and A/D interfaces. Fig. 1 presents a photograph of the experimental system. Since a load cell, rahter than displacement sensor, is applied to measure the displacement response, a calibration between the force and displacement is performed using laser interferometer.

To demonstrate hysteretic behaviors of the PSA-driven system, sinusoidal signal with different frequencies were adopted to excite the system and the results are presented in Fig. 2. It can be observed from Fig. 2 that loop structure between control voltage and displacement output is evident. It can also be found that the width of the hysteretic loop increases as the excitation frequency increases. The results were obtained from openloop experiments.

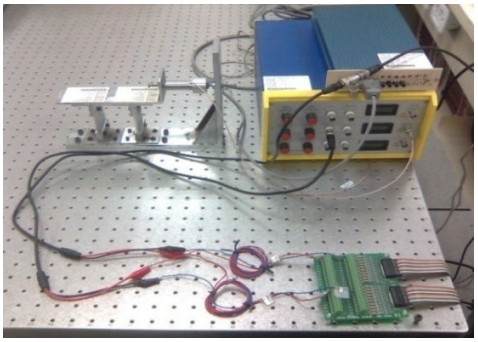


Fig. 1 A photograph illustrating the experimental set-up

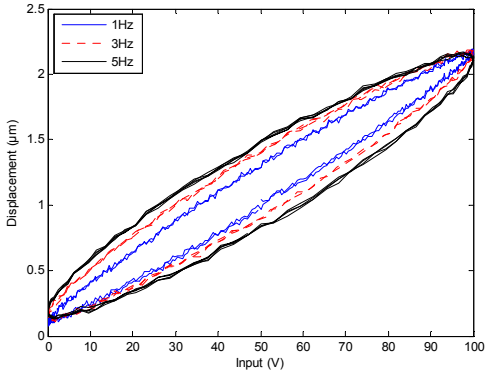


Fig. 2 Hysteretic behavior of the PSA-driven system

B. Hysteresis Identification using Bouc-Wen model

The Bouc-Wen model was originally proposed by Bouc in 1967 and later generalized by Wen in 1976. The model is suitable for the description of typical hysteresis [2]. Based on the structure of our PSA-driven system, the Bouc-Wen mathematical model can be expressed as

Open Science Index, Mechanical and Mechatronics Engineering Vol:8, No:3, 2014 publications.waset.org/9997810/pdf

$$m\ddot{x} + b\dot{x} + kx = k(d_1 u - h) \tag{7}$$

$$\dot{h} = \alpha d_1 \dot{u} - \beta|\dot{u}|h - \gamma \dot{u}|h| \tag{8}$$

where m, b, k separately represents the inertia, damping and stiffness of the PSA-actuated system while α, β, γ are the parameters used to determine the hysteretic loops' magnitude and shape. In addition, h is the hysteresis variable possessing dimension of displacement while d_1 is the piezoelectric constant representing a ratio between displacement output and control-voltage input. Based on the PSO and Bouc-Wen model, the hysteresis identification process becomes the following optimization problem

$$\underset{m,b,k,d,\alpha,\beta,\gamma}{\text{Min}} \; f(x) = \sqrt{\frac{\sum_{i=1}^{N} (x_e(i) - x(i))^2}{N}} \tag{9}$$

The optimization includes the equality constraints shown in (7) and (8) and the following inequality constraints

$$0 < b < \overline{b}; \;\; \underline{k} < k < \overline{k}; \;\; 0 < d_1 < \overline{d_1};$$
$$0 < \alpha < \overline{\alpha}; \;\; 0 < \beta < \overline{\beta}; \;\; 0 < \gamma < \overline{\gamma};$$

In the above, $f(x)$ is the objective or fitness function representing the root-mean-squares error between the experimental results, x_e, and their simulation counterparts, x. N is the total sampling number of the data, whereas under-bared and over-bared values separately indicate the lower and upper bounds of different model parameters. In accordance with the optimization problem described above, we provided searching ranges for different system parameters and then obtained optimized model parameters. The parameters identified are: $m = 0.75$; $b = 27.96$; $k = 8.54 \times 10^7$; $\alpha = 0.472$; $\beta = 0.072$; $\gamma = 0$; $d_1 = 2.15 \times 10^{-8}$ .Based on the identified model, a comparison between the experimental and simulated hysteresis can be performed and the results are presented in Fig. 3. One can readily find outfrom Fig. 3 that the identified model captures the system's hysteretic behavior well. The results presented correspond to 1-Hz sinusoidal excitation case.

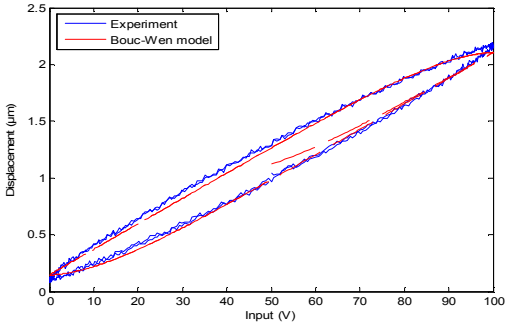


Fig. 3 Comparison of experimental and simulated hysteresis using the identified Bouc-Wen model

C. Hysteresis Identification using P-I model

Twenty input threshold values are configured in theinput span of [0,100] in the optimization problem associated with the P-I model. The input threshold vector can be represented as $\mathbf{r} = [r_1 \;\; r_2 \ldots \;\; r_n]^T$; $0 = r_1 < r_2 < \ldots\ldots < r_n$. The thresholds are organized in equal-distance manner. Moreover, the fitness function used in the Bouc-Wen case is also adopted here for the optimization process of the P-I parameters. To this end, twenty weights are identified and they are:

$$\mathbf{w}^T = [0.616, \;\; 0.285, \;\; -0.177, \;\; 0.221, \;\; 0.130, \;\; 0.044,$$
$$-0.238, \;\; 0.220, \;\; 0.085, \;\; 0.175, \;\; -0.203, \;\; -0.271,$$
$$0.115, \;\; -0.167, \;\; 0.380, \;\; -0.681, \;\; 0.500, \;\; -0.098,$$
$$0.364, \;\; -0.266]$$

By using the identified P-I hysteresis model, one can compare the experimental and simulated hysteresis. The results are presented in Fig. 4 in which the input signal is also 1-Hz sinusoidal whilethe experiments were done with open-loop control. According to Fig. 4 one can find out that identified P-I hysteresis model approximates the system's hysteresis better than the identified Bouc-Wen model.

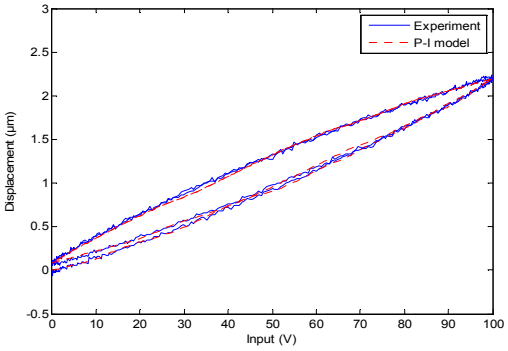


Fig. 4 Comparison of experimental and simulated hysteresis using the identified P-I model

IV. Feedforward Implementation in Motion Tracking

A. Feedforward-Control Implementation Based On the Identified Bouc-Wen Model

To eliminate the hysteresis nonlinearity, it is necessary to design a feedforward controller to cancel the nonlinear hysteretic behavior. However, the cancelation usually is not perfect. To compensate for this, a feedback control can be integrated with the feedforward control. In that regard, the resultant block diagram can be represented as Fig. 5.

Open Science Index, Mechanical and Mechatronics Engineering Vol:8, No:3, 2014 publications.waset.org/9997810/pdf

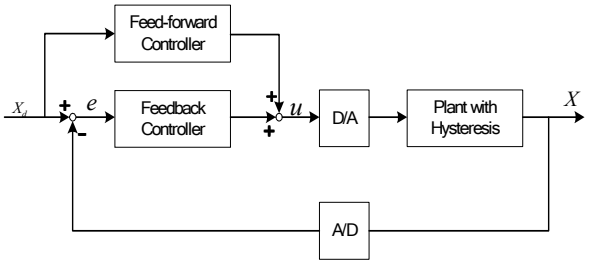


Fig. 5 The block diagram of the proposed control scheme

Two types of feedforward controller are designed in this study. First, a control design based on hysteresis estimate, rather than inverse hysteresis model, is adopted for the Bouc-Wen case. According to [2], the feedforward control in this case can be designed as the following expression

$$u_c = \frac{x_d(t) + \hat{h}(t)}{d_1} \tag{10}$$

where $\hat{h}(t)$ represents the estimate of hysteretic state varaible, $h(t)$. The hysteresis estimate can be computed in accordance with (8) and the identified parameters. When (10) is substituted into (7) the following can be obtained

$$m\ddot{x} + b\dot{x} + kx = k(d_1 \cdot x_d + \Delta) \tag{11}$$

where $\Delta = \hat{h} - h$ representing the difference between the estimated and true values of hysteresis variable. Based on (10) and (11) one can figure out that the hysteresis nonlinearity can be cancelled out if $\hat{h} \to h$. Note that $\hat{h}(t)$ is computed using the identified Bouc-Wen model. To verify the effectiveness of the proposed control scheme, motion tracking tasks were investigated. The verifications include stand-alone feedforward cancellation and feedforward-feedback scheme. To that end, Fig. 6 presents the tracking results using solely feedforward control while Fig. 7 presents the results obtained from feedforward-feedback scheme.

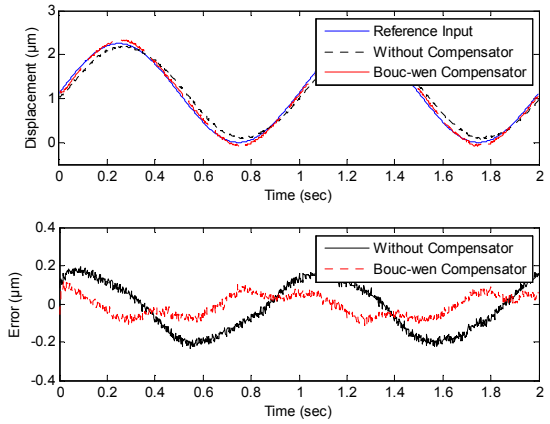


Fig. 6 1-Hz tracking by stand-alone Bouc-Wen feedforward control

It can be observed from Fig. 6 that although the feedfroward control can eliminate nonlinear hysteresis to some extent, the cancellation is not perfect. To complement for this, PID feedback compensation was adopted and the results are presented in Fig. 7. The control performance presented in Fig. 7 improves evidently. It turns out that the root-mean-squares error in 1-Hz tracking is 0.0577 and 0.0191μm for stand-alone feedforward and feedforward-feedback, respectively. The motion tracking investigations also include the 3-Hz and 5-Hz sinusoidal excitations. Tracking errors associated with these cases are listed in Table I. According to Table I one finds that similar trends exist in the 3-Hz and 5-Hz tracking cases. In other words, performances on direct feedforward cancellation seem not so perfect while feedforward-feedback control scheme improves the overall tracking performances substantially.

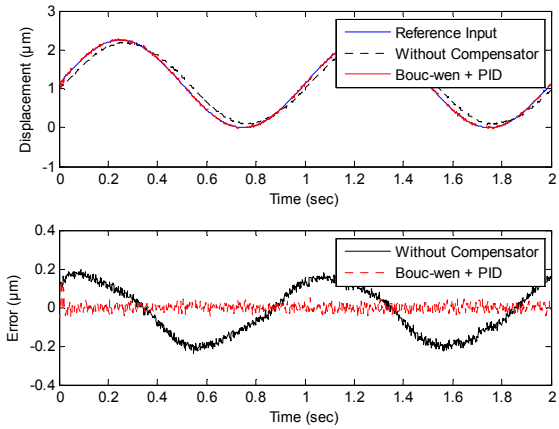


Fig. 7 1-Hz tracking by Bouc-Wen feedforward-feedback control

TABLEI
TRACKING PERFORMANCES OBTAINED BASED ON THE IDENTIFIED BOUC-WEN MODEL

Excitation	e_{max} (μm)	%	RMSE(μm)
1-Hz(feedforward)	0.198	8.8	0.0577
1-Hz(feedforward+feedback)	0.090	4.4	0.0191
3-Hz (feedforward)	0.337	15	0.0949
3-Hz(feedforward+feedback)	0.114	5.1	0.0258
5-Hz (feedforward)	0.459	20.4	0.1472
5-Hz (feedforward+feedback)	0.182	8.1	0.0427

B. Feedforward-Control Implementation Based On the Identified P-I Model

Unlike the approach adopted in the Bouc-Wen case where the hysteresis estimate, $\hat{h}$, is used to design the feedforward control input, the inverse P-I hysteresis model will be used in the P-I model case. Here the inverse P-I model was obtained from the identified P-I model. Since the P-I model has analytical inverse, the design of feedforward control becomes more straightforward than the Bouc-Wen case. Based upon the P-I model elaborated in (1)-(3), the inverse P-I model can be determined using the following equations

$$H^{-1}[y(k)] = \mathrm{w}'^{T} \cdot \mathrm{H}_{r'}[y, \mathrm{y}_0'](k) = \sum_{i=1}^{n} w_i' \cdot \max\{y(k) - r_i', \min\{y(k) + r_i', y'^{i}(k-1)\}\} \quad (12)$$

where

$$r_i' = \sum_{j=1}^{i} w_j (r_i - r_j), i = 1,2,\cdots n \quad (13)$$

$$y_{0i}' = \sum_{j=1}^{i} w_j y_{0i} + \sum_{j=i+1}^{n} w_j y_{0j}, i = 1, \ 2, \cdots \ n \quad (14)$$

$$w_1' = \frac{1}{w_1}, w_i' = -\frac{w_i}{(w_1 + \sum_{j=2}^{i} w_j)(\sum_{j=1}^{i-1} w_j)}, i = 2,3,\cdots n \quad (15)$$

Thus, the inverse P-I model can be determined if the weight vectors associated the P-I model were obtained. To this end, the weight vector associated with the inverse model were determined as the followings

$$\begin{aligned} \mathbf{w}'^{T} = [&1.834, \ -0.822, \ 0.148, \ 0.599, \ -0.525, \\ &-0.276, \ -0.046, \ 0.130, \ 0.324, \ 0.035, \\ &-0.443, \ -0.138, \ 0.271, \ -0.243, \ 0.070, \\ &0.034, \ -0.171, \ 0.306, \ -0.349, \ -0.110] \end{aligned}$$

Based on the inverse P-I model one can proceed to design the stand-alone feedforward control and feedforward-feedback control. Again, the effectiveness of the control schemes is verified by using sinusoidal trackings with frequency equal to 1, 3, 5 Hz while the results associated with 1-Hz case are presented in Figs. 8 and 9. Among these, Fig. 8 shows the results obtained from the stand-alone feedforward control, whereas Fig. 9 presents the counterparts of the feedforward-feedback control scheme.

Compare the results shown in Fig. 8 with that of Fig. 6, one can quickly find out that the hysteresis cancellation in Fig. 8 is better than that in Fig. 6. This indicates that the inverse P-I hysteresis approach can eliminate the hysteresis nonlinearity more effectively than the hysteresis-estimate approach based on the identified Bouc-Wen model. Such an observation can also be verified by checking the root-mean-squares error associated with these two control schemes. It turns out that the RMSE of the Bouc-Wen approach is 0.0577 μm while its counter part of the inverse P-I case is 0.0253 μm. Obviously, the inverse P-I approach outperforms the approach based on the identified Bouc-Wen model.

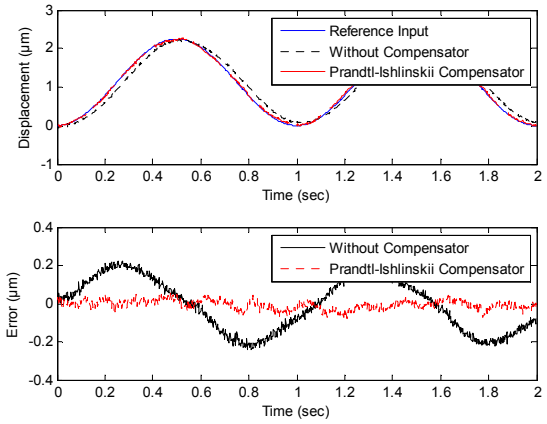


Fig. 8 1-Hz tracking by stand-alone inverse P-I feedforward control

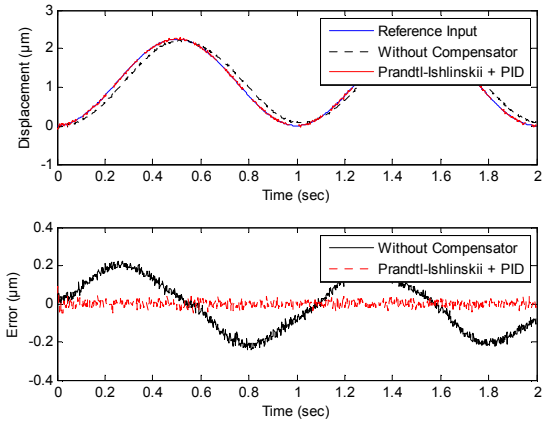


Fig. 9 1-Hz tracking by inverse P-I feedforward-feedback control

In order to further improve tracking performances, traditional PID control scheme is integrated with the inverse P-I feedforward control and the results are shown in Fig. 9. Compare the results of Fig. 9 with that of Fig. 8, one can observe that only slight improvement has been accomplished this case. This is because the direct cancellation using stand-alone inverse P-I control is already quite good. Similar trends can also be observed in 3- and 5-Hz tracking cases. To verify this, tracking performances corresponding to solely feedforward and feedforward-feedback control are listed in Table II. Based on the results of Tables I and II, one can conclude that inverse P-I model can effectively eliminate the nonlinear hysteresis behavior of the PSA-driven system while the approach adopted in the Bouc-Wen case seems not as efficient as the inverse P-I case.

TABLEII
TRACING PERFORMANCES OBTAINED BASED ON THE IDENTIFIED P-I MODEL

Excitation	e_{max} (μm)	%	RMSE (μm)
1-Hz(feedforward)	0.124	5.5	0.0253
1-Hz(feedforward+feedback)	0.074	3.3	0.0162
3-Hz (feedforward)	0.164	7.3	0.0378
3-Hz(feedforward+feedback)	0.133	5.9	0.0243
5-Hz (feedforward)	0.204	9.1	0.0533
5-Hz (feedforward+feedback)	0.155	6.9	0.0292

Open Science Index, Mechanical and Mechatronics Engineering Vol:8, No:3, 2014 publications.waset.org/9997810/pdf

Open Science Index, Mechanical and Mechatronics Engineering Vol:8, No:3, 2014 publications.waset.org/9997810/pdf

V. Conclusion

This paper investigates tracking problems of a PSA-driven system. Two hysteresis models including Bouc-Wen and Prandtl-Ishlinskii model are adopted to design feedforward control so that nonlinear hysteresis effect of the system can be directly eliminated. Due to the complexity of the hysteresis models, particle swarm optimization (PSO) algorithm is applied to search for optimal hysteresis model parameters so that nonlinear hysteresis features can be precisely represented. A feedforward control based on the hysteresis estimate obtained from the identified Bouc-Wen model is designed to handle sinusoidal tracking tasks. The tracking results are compared with those obtained from another feedforward design based on inverse P-I model. It turns out that the hysteresis cancellation using inverse P-I model performs better than the design using the hysteresis estimate of the identified Bouc-Wen model. Traditional PID control scheme is integrated with both feedforward control designs to further improve the tracking performances.

Acknowledgment

The authors appreciate financial support from National Science Council, Taiwan,ROC under Grant NSC 102-2221-E-131-010.

References

[1] Q. Xu and P.-K. Wong, "Hysteresis modeling and compensation of a piezostage using least squares support vector machines," *Mechatronics*, vol. 21, pp. 1239-1251, 2011.

[2] C.-J. Lin and P.-T. Lin, "Particle swarm optimization based feedforward controller for a XY PZT positioning stage," *Mechatronics*, vol.22, pp.614-628, 2012.

[3] P.-K. Wong and Q. Xu, "Rate-dependent hysteresis modeling and control of a piezostage using online support vector machine and relevance vector machine," *IEEE Trans. Industrial Electronics*, vol. 59, no.4, pp.1988-2001, 2012.

[4] W. Li and X. Chen, "Compensation of hysteresis in piezoelectric actuators without dynamics modeling," *Sensors and Actuators A*: Physical, vol. 199, pp.89-97, 2013.

[5] W. T. Ang, K. Khosla and C. N. Riviere, "Feedforward controller with inverse rate-dependent model for piezoelectric actuators in trajectory-tracking applications," *IEEE/ASME Trans. Mechatronics*, vol. 12, no. 2, 2007.

[6] I. D. Mayergoyz, *ThePreisach model for hysteresis*, Berlin: Springer, 1991.

[7] I. D. Mayergoyz, "Dynamic Preisach models of hysteresis," *IEEE Trans. Magn*, vol. 24, pp.2925-2927, 1988.

[8] R. Bouc, "Forced vibration of mechanical systems with hysteresis," In: 4th*International Conference on Nonlinear Oscillation*, 1967.

[9] Y. K. Wen, "Method of random vibration of hysteretic systems," *Journal of Engineering Mechanics*, vol. 102, pp.249-263, 1976.

[10] X. Zhang, Y. Huang, J. Liu, X. Wang and F. Gao, "A method identifying the parameters of Bouc-Wen hysteresis nonlinear model based on genetic algorithm,"*Intell. Process Syst.*, pp.662-665, 1997.

[11] Y. Bazi, "Semisupervised PSO-SVM regression for biophysical parameter estimation," *IEEE Trans. Geoscience and Remote Sensing*, vol. 45, no. 6, pp. 1887-1895, 2007.

[12] M. Marinaki, Y. Marinakis and G. E. Stavroulakis, "Vibration control of beams with piezoelectric sensors and actuators using particle swarm optimization," *Expert Systems with Applications*, vol. 38, pp.6872-6883, 2011.

[13] C.-C. Kao and R.-F. Fung, "Using the modified PSO method to identify a Scott-Russell mechanism actuated by a piezoelectric element," *Mechanical Systems and Signal Processing*, vol. 23, pp.1652-1661, 2009.

[14] M.-J. Yang, G.-Y. Gu and L.-M. Zhu, "Parameter identification of the generalized Prandtl-Ishlinskii model for piezoelectric actuators using modified particle swarm optimization," *Sensors and Actuators A: Physical*, vol. 189, pp. 254-265, 2013.